

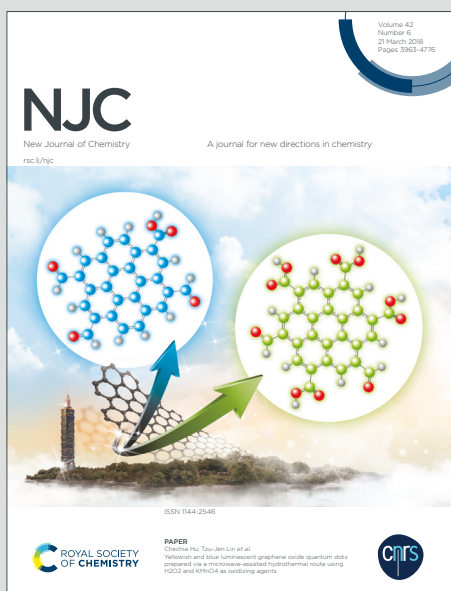
NJC

New Journal of Chemistry

A journal for new directions in chemistry

Accepted Manuscript

This article can be cited before page numbers have been issued, to do this please use: R. W. Jadhav, D. D. La, T. Ngoc Truong, S. V. Khalap, V. Q. Dang and S. V. Bhosale, *New J. Chem.*, 2020, DOI: 10.1039/D0NJ03355C.



This is an Accepted Manuscript, which has been through the Royal Society of Chemistry peer review process and has been accepted for publication.

Accepted Manuscripts are published online shortly after acceptance, before technical editing, formatting and proof reading. Using this free service, authors can make their results available to the community, in citable form, before we publish the edited article. We will replace this Accepted Manuscript with the edited and formatted Advance Article as soon as it is available.

You can find more information about Accepted Manuscripts in the [Information for Authors](#).

Please note that technical editing may introduce minor changes to the text and/or graphics, which may alter content. The journal's standard [Terms & Conditions](#) and the [Ethical guidelines](#) still apply. In no event shall the Royal Society of Chemistry be held responsible for any errors or omissions in this Accepted Manuscript or any consequences arising from the use of any information it contains.

ARTICLE

The controllable nanostructure and photocatalytic behaviour of 5,10,15,20-tetra-(3,4,5 trimethoxyphenyl) porphyrin through solvophobic supramolecular self-assembly

Received 00th January 20xx,
Accepted 00th January 20xx

DOI: 10.1039/x0xx00000x

Ratan W. Jadhav,^a Duong Duc La,^b Tuan Ngoc Truong,^b Shambhu V. Khalap,^a Dang Viet Quang,^{c,*} Sheshanath V. Bhosale^{a,*}

In this study, the self-assembly of 5,10,15,20-tetra(3,4,5-trimethoxyphenyl)porphyrin (coded as: **TTOP**) in the mixture of tetrahydrofuran (THF) and H₂O and the photocatalytic activity of resulting self-assembled aggregates toward the degradation of organic compounds were investigated. **TTOP** were well dispersed as monomers in THF, however, they stacked into aggregates upon the addition of water (20–90%). Depending on the THF/H₂O mixture various nanostructures were observed. Microrods with an average width of 0.62±0.22 μm and length of 10.17±2.04 μm and the sphere-like particles with diameters ranging from 0.5 to 1.2 μm were obtained in 70% water in THF. Nonetheless, the particles disappeared and rods turned to slabs with same length but much larger width (4.48±2.27 μm) as 80% water in THF was used. The particles with irregular shapes, which connected into large aggregates, were obtained at 90% water in THF. These structures exhibited significant difference in photocatalytic ability for the degradation of dye (rhodamine B, RhB and methylene blue, MB). The rate constants of RhB degradation were 4.35·10⁻⁴ min⁻¹, 1.13·10⁻³ min⁻¹, 2.63·10⁻³ min⁻¹, and 3.52·10⁻³ min⁻¹ for the porphyrin monomers in THF and its aggregates states obtained by mixing of 70%, 80%, and 90% water in THF, respectively. The results indicated the important role of solvent in the formation and control the structures of porphyrin aggregates, which are crucial to an effective porphyrin-based photocatalyst.

Introduction

Porphyrin and its derivatives possess very unique physicochemical properties,^{1,2} which can be significantly varied by the attachment of functional groups on macrocycles and/or by chelation with metal ions in the center of macrocycles. The attachment of organic moieties e.g. hydrogen bonding motifs and exocyclic ligands allows porphyrins to self-assemble into various supramolecular nanomaterials.^{3,4} The porphyrin self-assembly is based on physical interactions such as hydrogen bonding, van der Waals interaction, and π-π interaction. The porphyrin self-assembled nanomaterials show a great photocatalytic activity, which has recently drawn significant attention.

Porphyrin derivatives such as TiO₂-porphyrin and metal-porphyrins show highly photocatalytic activity for photosynthesis and photodegradation of organic compounds, CO₂ reduction, water splitting.^{1,3,5-15} Singh et al. developed a self-assembled carbon nitride/cobalt porphyrin, which has been successfully applied as photocatalyst for selective production of L-glutamate and α-ketoglutarate. Zhang et al. have demonstrated the high H₂ and O₂

evolution (40.8 and 36.1 mmol/g⁻¹h⁻¹) by using metal-free porphyrin supramolecular nanomaterial as photocatalyst.⁹ Porphyrin nanomaterials show a great potential for CO₂ conversion.¹⁶ The system of iron porphyrins and phenoxazine-based organic photosensitizer converted CO₂ to CO and CH₄ with the turnover number (TON) of 149 and 29, respectively, by the irradiation of visible light (λ>430 nm). Won et al. revealed that a Zn-porphyrin/TiO₂/Re catalyst can offer an effective CO₂ to CO reduction with the TON upto 1000 in 42 h.¹⁷

In the past, metal-porphyrins were frequently investigated as photocatalysts.^{3,18} However, recently the investigation of metal-free porphyrins as photocatalysts has been of interest. Several nanomaterials based on self-assembled supramolecular metal-free porphyrins have been explored as photocatalysts for oxidation reaction such as water splitting and the degradation of organic compounds. The self-assembled supramolecular metal-free porphyrin nanomaterials are usually obtained by grafting different functional groups on porphyrin macrocycles and self-assembling in a mixture of good and poor solvents or by changing the pH. By grafting 4-pyridyl, 4-cyanophenyl or 4-carboxyphenyl groups on porphyrin macrocycle, Zhang group demonstrated that 5,10,15,20-tetra-(4-carboxyphenyl)porphyrin (TCPP) has better photodegradation activity toward phenol compounds compared to C₃N₄ and Bi₂WO₆.⁹ The photocatalytic activity of TCPP is greatly affected by the structures of self-assemblies. Lu et al. indicated that self-assembled TCPP showed higher catalytic activity for phenol degradation than its powder form and that for the aggregates of nanorods were better than nanofibers.¹² In another study, La et al. also showed the enhanced catalytic activity of TCPP in the form of

^a School of Chemical Sciences, Goa University, Taleigao Plateau, Goa-403 206, India.

E-mail: svbhosale@uniqoa.ac.in

^b Institute of Chemistry and Materials, Hanoi 100000, Viet Nam.

^c Faculty of Biotechnology, Chemistry and Environmental Engineering, Phenikaa University, Hanoi 12116, Vietnam.

E-mail: quang.dangviet@phenikaa-uni.edu.vn

† Footnotes relating to the title and/or authors should appear here.

Electronic Supplementary Information (ESI) available: [details of any supplementary information available should be included here]. See DOI: 10.1039/x0xx00000x

nanobelt structure with 90% rhodamine B (RhB) degraded in 3h.¹³ The self-assemblies of protoporphyrin with L-/D-arginine generated a rose-like nanostructure, which can degrade 78-80% RhB under sunlight irradiation for 340 min.¹⁵ Aljabri *et al.* grafted pentafluorophenyl groups to form 5,10,15,20-tetra (pentafluorophenyl)porphyrin (TPFP) and examined its photodegradation activity against RhB.¹⁴ They revealed that TPFP can be assembled in the mixture of THF and H₂O to form aggregates of microrods or octahedral crystals, which both had a good photocatalytic activity for the degradation of RhB with rate constants of 3.76×10^{-3} and $2.93 \times 10^{-3} \text{ min}^{-1}$, respectively. Obviously, porphyrin-based nanomaterials could become promising photocatalysts by modifying the macrocycle with various functional groups without the addition of any co-catalyst. Functional groups attached onto porphyrin macrocycle play utmost important role on the properties and photocatalytic activity of the resulting nanomaterials. Even though, porphyrins have been modified with several functional groups, the functionalization of porphyrin to its periphery with trimethoxyphenyl group for photocatalyst has never been investigated. Therefore, this study will fabricate the supramolecular nanostructures of 5,10,15,20-tetra (3,4,5-trimethoxyphenyl) porphyrin (TTOP, Figure 1 a) in THF/H₂O solvent and investigate their photocatalytic ability for the degradation of RhB.

Results and Discussion

Self-assembly behavior of TTOP in THF/H₂O solvent

TTOP monomer is highly soluble in THF solvent, which showed a strong absorption at 420 nm on UV-Vis spectrum (Figure 1 b) due to the characteristic $\pi-\pi^*$ transition on the porphyrin structure. Besides the strong absorption at 420 nm belonging to the electron transfer from ground state (S_0) to the second excited state (S_2), the electronic absorption spectra for TTOP showed other four Q bands at 514, 549, 593, and 649 nm corresponding to the electron transition from ground state, S_0 to the first excited state, S_1 .¹⁹ The intensity of these absorption bands decreased upon the addition of increasing water percentage (20 to 90%) into the solvent indicating the occurrence of the TTOP self-assembly. According to recent studies, the porphyrin macrocycle aggregation in a mixture of good and poor solvents has been considered as a major mechanism for the self-assembly of porphyrin supramolecular nanomaterials.^{9, 20} The addition of a poor solvent, in which porphyrins are insoluble, into a good solvent in which porphyrins are well dissolved resulting in the formation of supramolecular aggregates. The aggregates are usually formed through non-covalent bonds such as the $\pi-\pi$ stacking, hydrogen bonding, ligand coordination, or/and spatial arrangement of porphyrins. Based on the molecular structure of TTOP as shown in Figure 1 a, it can be deduced that the $\pi-\pi$ stacking should be a major interaction leading to the formation of TTOP supramolecular aggregates.

To further investigate the possible bonds that may contribute to the formation of aggregates, the FTIR spectra of TTOP in THF and the aggregates in H₂O/THF have been collected for an evaluation. As can be seen in their FTIR spectra (Figure 2), except some peaks belong to water at 1630 cm^{-1} and 3400 cm^{-1} , no new peak was detected for the aggregates in H₂O/THF solvent. This observation indicated that the formation of TTOP aggregates is based on the

non-covalent bond, particularly the $\pi-\pi$ stacking interaction. These results revealed that TTOP macrocycles formed J-aggregates through $\pi-\pi$ stacking interaction in a head to tail fashion and perfectly matches with literature.²¹

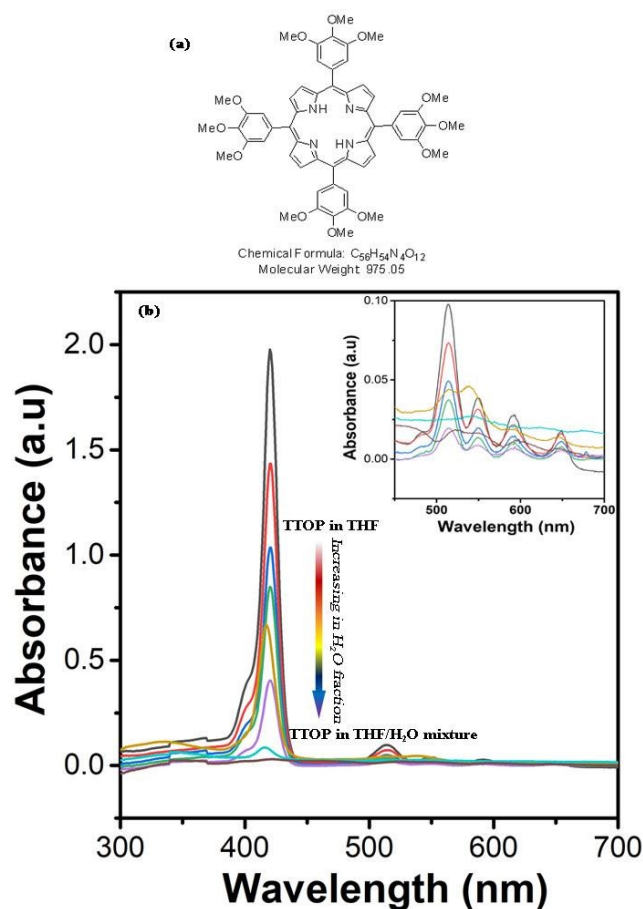


Figure 1. Molecular structure of TTOP porphyrin (a) and UV-vis spectra of TTOP in THF upon addition of water fraction 20-90% as shown in (b), respectively. Inset is enlarged UV-vis spectra at the range of 450–700nm.

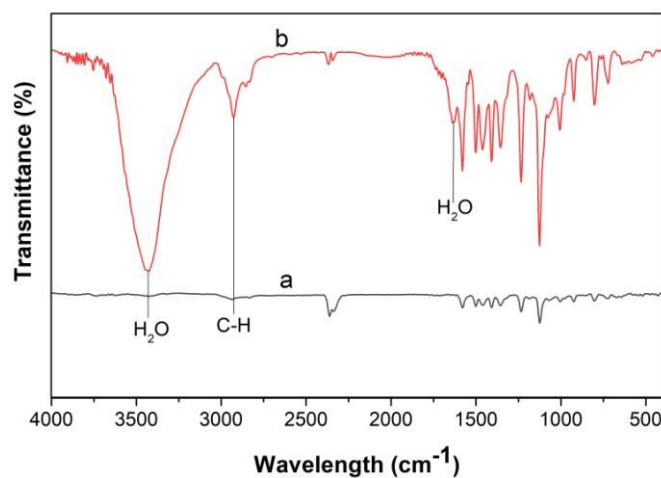


Figure 2. FTIR spectra of TTOP porphyrin in THF (a) and TTOP aggregates in THF/H₂O mixture (b).

The effect of water on the optical properties of **TTOP** was further studied by the photoluminescence (PL) spectroscopy. The PL spectra were attained by the excitation at 420 nm and results are shown in **Figure 3**. Two distinct emission peaks were observed at 662 nm and 727 nm on the spectrum of **TTOP** in THF solvent. The quenching in photoluminescence was apparently observed as the water was added into the solution. The luminescence became weakened with the increasing water fraction and almost completely quenching at 90% water; this further confirmed the aggregation of **TTOP** macrocycles.

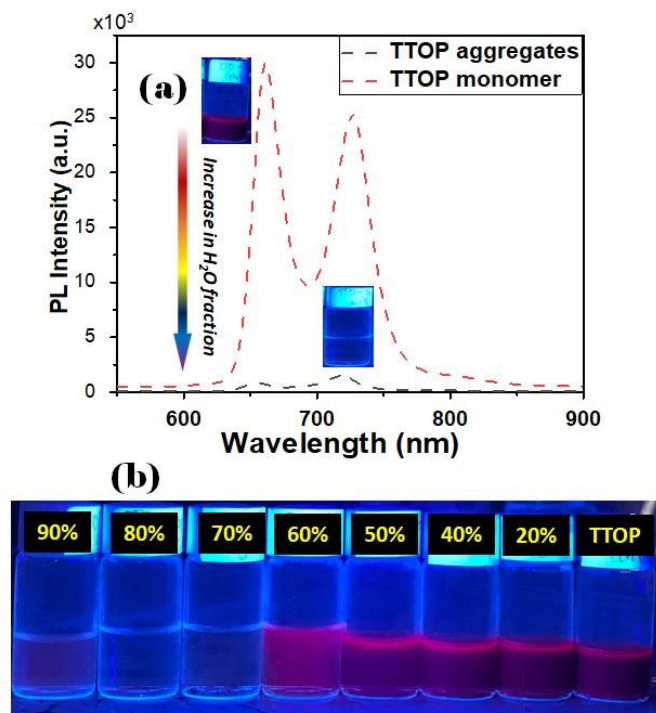


Figure 3. PL spectra of **TTOP** in THF and with water fraction of 90% (a), and optical images of **TTOP** aggregates in THF with different water fractions (b).

The formation of **TTOP** supramolecular aggregates can be observed on SEM images exhibited in **Figure 4**. At the water fraction of 70%, a mixture of microrods and sphere-like particles was obtained (**Figure 4 a**) in which microrods are $0.62 \pm 0.22 \mu\text{m}$ in width and $10.17 \pm 2.04 \mu\text{m}$ in length and the particles have diameters ranging from 0.5 to 1.2 μm , respectively. When the water fraction increased to 80%, the sphere-like particles disappeared and slabs with the similar length of above microrods ($10.57 \pm 4.37 \mu\text{m}$) were received; but, the width enlarged significantly to $4.48 \pm 2.27 \mu\text{m}$ (**Figure 4 b**). At the water fraction above 90%, the particles with irregular shapes tending to fuse into large aggregates were obtained. Those aggregates are relatively stable; their size and shape were not changed after being used in photocatalytic reaction as exhibited in **Figure S1**. Just to see whether **TTOP** further influence with 95% water in THF, it can be clearly seen that only small particular aggregates observed. The variation in shapes and sizes with the $\text{H}_2\text{O}/\text{THF}$ ratios was most likely due to the variation in the solubility of **TTOP** in the solvent mixture, which influenced the creation of crystalline nuclei and the

growth process. As seen in **Figure 4**, the solvent with 80% water produced higher crystalline **TTOP** nanomaterials compared to the others and this was aligned with the observation on XRD spectra in **Figure S2**. No diffraction peak was presented in the XRD pattern of the **TTOP** monomers, which indicates that monomeric **TTOP** molecule is amorphous in nature. Whereas, sharp peaks at about 20.1° , 26.3° , and 46.9° were found on the XRD patterns of the **TTOP** aggregates produced in the THF/ H_2O mixtures at the water fraction of 70% and 80%. These peaks are attributed to the crystalline structure of self-assembled **TTOP**, indicating that π - π stacking and electrostatic interactions lead to the formation of well-ordered crystals of the **TTOP** molecules in the THF/ H_2O mixture. These results indicated that the **TTOP** supramolecular nanomaterials were successfully synthesized by the addition of water into the solvent. The size and shape of the resulting nanomaterial can be controlled by tuning the H_2O fraction in solvent mixture.

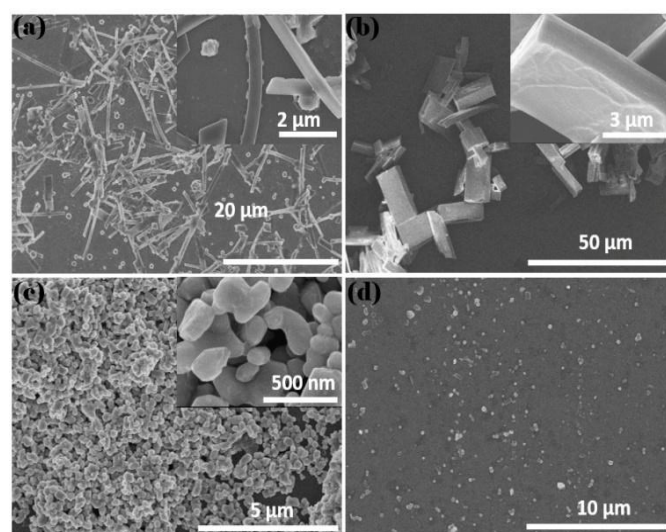


Figure 4. SEM image of **TTOP** porphyrins self-assembled in THF with different water fractions of a) 70%, b) 80%, c) 90%, and d) 95%.

The photocatalytic activity

Porphyrins have a structure that is similar to chlorophyll, a natural photoactive molecule with strong photocatalytic activity in plant and algae. Thanks to the structural similarity, porphyrins and their assembled nanomaterials possess a photocatalytic activity and they have been extensively exploited as photocatalyst for the degradation of organic compound contaminants under the visible light. Based on the UV-Vis spectra, the energy bandgap for **TTOP** self-assembled supramolecular nanomaterial was calculated to evaluate its potential application for photocatalytic reaction. **TTOP** porphyrin and assembled aggregates have a bandgap of $\approx 2.85 \text{ eV}$ that indicated the possible photoactivity of this nanomaterial in the visible light.

The photocatalytic activities of **TTOP** monomer and assembled nanomaterial were experimentally evaluated through the degradation of RhB dye under the visible light irradiation. The concentration of RhB was determined based on UV-Vis absorption at the wavelength of 553 nm. The removal efficiency of RhB by the photodegradation are shown in **Figure 5 a**. Slight change (5.1%) was

observed after the RhB solution (without photocatalyst) was irradiated with visible light at wavelength of 420 nm for 360 min. This indicated that the self-photodegradation of RhB was insignificant. Meanwhile, 14.5% RhB was degraded at the same irradiation period as the **TTOP** monomer was added. This revealed an apparent photocatalytic activity induced by **TTOP** molecules. Interestingly, the RhB degradation increased considerably with the utilization of **TTOP** self-assembled nanomaterials. **TTOP** aggregates prepared by using solvent with 70% water can degrade 38.7% RhB after 360 min irradiation. Surprisingly, the degradation efficiency sharply increased to 65.0% and 70.8% with **TTOP** aggregates synthesized by using solvent with 80% and 90% water, respectively. This photocatalytic behaviour was also observed as Methylene blue (MB) was used in place of RhB. Negligible MB degradation was observed in the absence of **TTOP** aggregates (Figure S3), which implies that the self-sensitized photodegradation of MB does not occur readily under these. The **TTOP** aggregates show a remarkable photocatalytic performance toward MB under visible light irradiation. The MB removal percentage reached 38, 68, and 74%, when **TTOP** aggregates were produced in THF/H₂O mixtures with the water fraction of 70, 80, and 90%, respectively. This observation confirmed that the formation of supramolecular materials helps improve catalytic activity of **TTOP** porphyrin. Higher photocatalytic activity of **TTOP** aggregates synthesized by using solvent with 80% and 90% water compared to the one with 70% water could be resulted from the differences in their shape and size. 70% Water produced a mixture of microrods and sphere-like particles, 80% water generated highly crystalline slabs, and meanwhile, 90% water favored the formation of irregular shaped particles which interconnected to large aggregates. This interconnected **TTOP** self-assembled nanomaterials could adsorb more RhB resulting in higher photocatalytic performance.

The kinetics of photocatalytic degradation was investigated based on the first-order kinetic equation (Eq. 1).

$$r = -\frac{dC}{dt} = kC \quad (1)$$

where, *r* is reaction rate, *C* is RhB concentration, *t* is reaction time, and *k* is first-order rate constant. Applying the boundary conditions: *t*=0, *C*_t=*C*₀ is the initial RhB concentration, it has an integrated form as follows:

$$\ln\left(\frac{C_t}{C_0}\right) = -kt \quad (2)$$

Linear plot of $\ln(C_t/C_0)$ vs time (*t*) allows one to determine reaction rate constant, *k*. Here, the light absorption intensity of RhB solution at 553 nm at the beginning and at time *t* can be used instead of actual concentration. In this study, the plots of $\ln C_t/C_0$ vs *t* is shown in Figure 5 b. The rate constant of the RhB degradation by **TTOP** monomer, and aggregates in 70%, 80%, and 90% water solvent were $4.35 \cdot 10^{-4} \text{ min}^{-1}$, $1.13 \cdot 10^{-3} \text{ min}^{-1}$, $2.63 \cdot 10^{-3} \text{ min}^{-1}$, and $3.52 \cdot 10^{-3} \text{ min}^{-1}$, respectively. These results confirmed that the photocatalytic activity was significantly improved when porphyrin monomer transformed into aggregate forms. This similar trend was also observed in other metal-free porphyrins.^{13, 22} The variation in the rate of RhB photodegradation by **TTOP** assembled aggregates obtained in different water fraction is likely due to their differences in the shape and size.²³ The RhB photodegradation rate of **TTOP** self-assembled aggregates is comparable to some other porphyrin aggregates, 5,10,15,20-tetrakis(pentafluorophenyl)porphyrin

aggregates self-assembled in THF/H₂O(70% water)¹⁴ and tetrakis(4-carboxyphenyl) porphyrin aggregates¹³ with rate constant of $3.76 \cdot 10^{-3} \text{ min}^{-1}$ and $3.9 \cdot 10^{-3} \text{ min}^{-1}$, respectively. It is also slightly higher than that for P-25 Degussa TiO₂ ($2.2 \cdot 10^{-3} \text{ min}^{-1}$).¹³

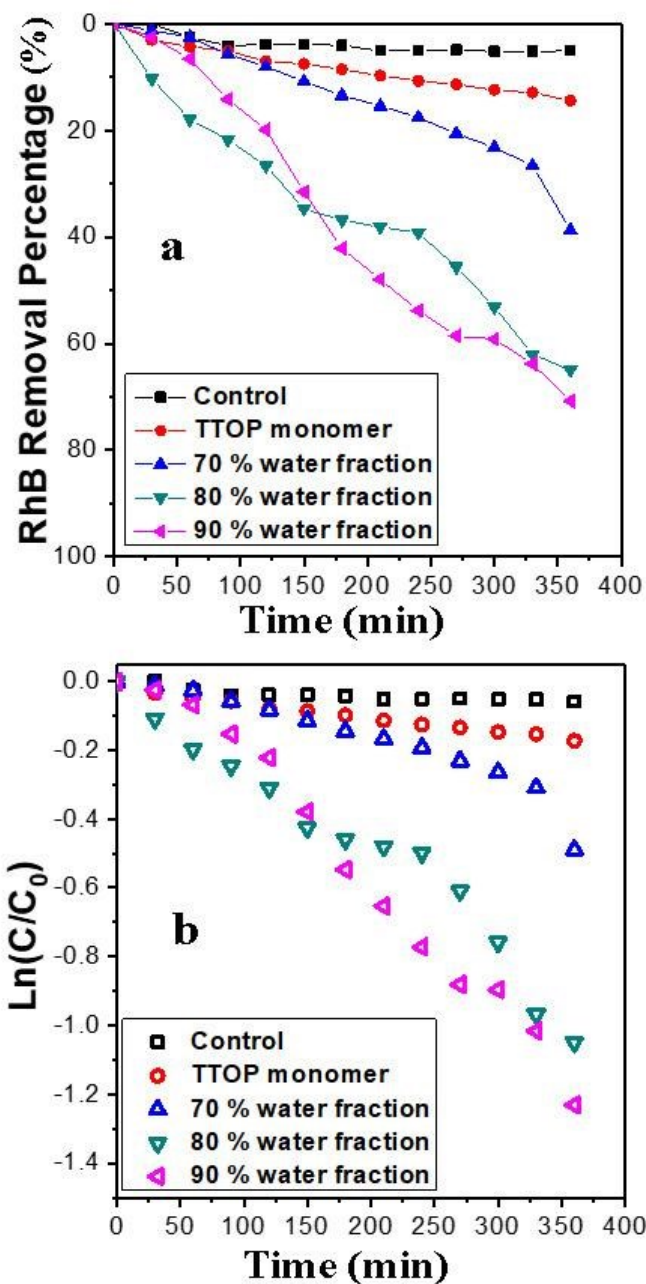
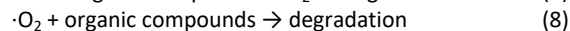
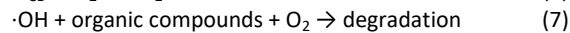
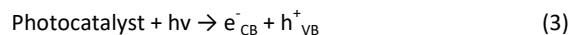


Figure 5. Photocatalytic behaviour of **TTOP** porphyrin aggregates toward Rhodamine B dye: a) removal efficiency and b) photodegradation kinetics.

As discussed in previous works, the RhB degradation by porphyrins and their derivatives is due to the oxidation caused by the holes and oxidative radicals that are generated upon the visible light irradiation.^{13, 14, 22} The key to an efficient photocatalyst is its ability to generate electron/hole couples in which electron and hole (charges) can be separately existed long enough for the redox reaction as shown in Eq. 3–8. The charges are generated due to the jump of electrons (negative charges) from the highest occupied to

the lowest unoccupied molecular orbitals (HOMO and LUMO, respectively) leaving behind holes (positive charges). When the molecules are far from each other, the charge transfer is dominated by an intramolecular process. However, when the HOMO and LUMO orbitals of neighboring molecules are in the close distance of few angstroms ($\approx 3.5\text{--}4 \text{ \AA}$, such as the distance found in molecular π -stacks²⁴) and overlapped, intermolecular charge transfer process may occur and which could enhance the electron/hole separation.



In this study, **TTOP** molecules dispersed in the THF solvent, they could exist as single molecules that randomly collide and contact and therefore the charge transfer is likely based mainly on intramolecular process. Since there is a lack of strong charge withdrawal group on **TTOP** molecule, the electron/hole couples could be recombined quickly and this could be a reason for the lower photocatalytic performance of **TTOP** solution. The situation, however, was different as **TTOP** porphyrins assemble into the J-type aggregates through the π - π interaction. The charge transfer could occur via intermolecular process. Once electrons and holes are separated, they are more difficult to recombine than in the intramolecular charge transfer process because of the deflection on **TTOP** supramolecular crystals, which increase the lifetime of charges. Accordingly, the higher structural disorder degree found in porphyrin aggregates can generate charge with longer lifetime and this could be the explanation to the higher RhB photodegradation of the aggregates received by 90% water solvent. The observation in this study is in congruence with previous works on different types of the self-assembled porphyrins revealing the utmost importance of the shape control in photocatalytic performance of porphyrin aggregates.^{13, 14, 22}

To demonstrate the roles of $\cdot\text{OH}$, $\cdot\text{O}_2^-$ and hole (h^+) free radicals for the RhB degradation process on the surface of the **TTOP** aggregates, three radical trapping agents including isopropanol, ammonia oxalate, and benzoquinone were used to trap $\cdot\text{OH}$, h^+ , and $\cdot\text{O}_2^-$ radicals, respectively.¹² The results are shown in **Figure 6**. It can be clearly seen from the figure that with the presence of the radical scavengers, the RhB degradation efficiencies are significantly decreased in comparison to that without radical scavengers. After 90 minutes of irradiation, the RhB removal percentage decreases from 74.8% to 64.2, 32.3, and 20.7% upon addition of isopropanol, ammonia oxalate, and benzoquinone, respectively. This can be concluded that the $\cdot\text{OH}$, $\cdot\text{O}_2^-$, and hole (h^+) free radicals play an important role for the degrading process of RhB using **TTOP** aggregates as photocatalyst.

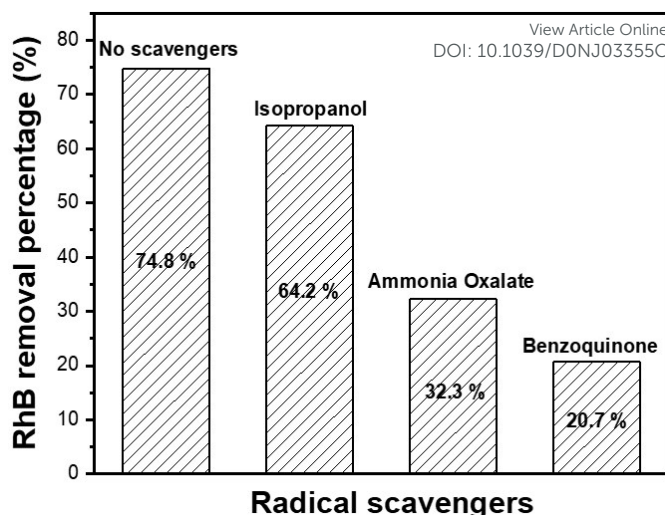


Figure 6. Effect of radical intermediate trapping agents on the removal efficiency of RhB upon the visible light irradiation

Conclusion

Supramolecular nanomaterials of **TTOP** porphyrin were successfully synthesized by self-assembly in THF/H₂O solvent. The shape and size of aggregates can be easily controlled by tuning the THF/H₂O ratio. 70% Water produced a mixture of microrods ($0.62 \pm 0.22 \mu\text{m}$ in diameter and $10.17 \pm 2.04 \mu\text{m}$ in length, respectively) and sphere-like nanoparticles (diameters in a range of 0.5 to 1.2 μm). These particles disappeared meanwhile the diameter of microrod increased significantly to about $4.48 \pm 2.27 \mu\text{m}$ at the water fraction of 80%. Interestingly, this highly ordered structure was completely transformed to irregularly shaped particles, which tend to flocculate into large and porous aggregates. These differences in shapes and sizes caused a great variation in the photocatalytic activity of resulting self-assembled TTO aggregates. The rate constants of RhB photodegradation were $4.35 \cdot 10^{-4} \text{ min}^{-1}$, $1.13 \cdot 10^{-3} \text{ min}^{-1}$, $2.63 \cdot 10^{-3} \text{ min}^{-1}$, and $3.52 \cdot 10^{-3} \text{ min}^{-1}$ for **TTOP** monomer, and aggregates formed by 70%, 80%, and 90% water solvent, respectively. This result indicated that the photocatalytic performance of **TTOP** porphyrin can be enhanced by the transformation of monomers to self-assembly forms and further improvement can be achieved by the control of size and morphology of assembled aggregates.

Conflicts of interest

There are no conflicts to declare

Acknowledgements

This research is funded by Vietnam National Foundation for Science and Technology Development (NAFOSTED) under grant number 104.05-2019.01. S.V.B. (GU) acknowledges University Grants Commission-Faculty Recharge Program (India) for award of Professorship.

References

1. Wang, J.; Zhong, Y.; Wang, L.; Zhang, N.; Cao, R.; Bian, K.; Alarid, L.; Haddad, R. E.; Bai, F.; Fan, H., Morphology-Controlled Synthesis and Metalation of Porphyrin Nanoparticles with Enhanced Photocatalytic Performance. *Nano Letters* **2016**, *16* (10), 6523-6528.

ARTICLE

Journal Name

2. Min Park, J.; Lee, J. H.; Jang, W.-D., Applications of porphyrins in emerging energy conversion technologies. *Coordination Chemistry Reviews* **2020**, *407*, 213157.
3. Drain, C. M.; Varotto, A.; Radivojevic, I., Self-Organized Porphyrinic Materials. *Chemical Reviews* **2009**, *109* (5), 1630-1658.
4. Liu, C.; Liu, K.; Wang, C.; Liu, H.; Wang, H.; Su, H.; Li, X.; Chen, B.; Jiang, J., Elucidating heterogeneous photocatalytic superiority of microporous porphyrin organic cage. *Nature Communications* **2020**, *11* (1), 1047.
5. Duc La, D.; Rananaware, A.; Nguyen Thi, H. P.; Jones, L.; Bhosale, S. V., Fabrication of a TiO₂@porphyrin nanofiber hybrid material: a highly efficient photocatalyst under simulated sunlight irradiation. *Advances in Natural Sciences: Nanoscience and Nanotechnology* **2017**, *8* (1), 015009.
6. Tian, S.; Chen, S.; Ren, X.; Cao, R.; Hu, H.; Bai, F., Bottom-up fabrication of graphitic carbon nitride nanosheets modified with porphyrin via covalent bonding for photocatalytic H₂ evolution. *Nano Research* **2019**, *12* (12), 3109-3115.
7. Kumar, S.; Wani, M. Y.; Arranja, C. T.; e Silva, J. d. A.; Avula, B.; Sobral, A. J. F. N., Porphyrins as nanoreactors in the carbon dioxide capture and conversion: a review. *Journal of Materials Chemistry A* **2015**, *3* (39), 19615-19637.
8. Liu, Y.; Wang, L.; Feng, H.; Ren, X.; Ji, J.; Bai, F.; Fan, H., Microemulsion-Assisted Self-Assembly and Synthesis of Size-Controlled Porphyrin Nanocrystals with Enhanced Photocatalytic Hydrogen Evolution. *Nano Letters* **2019**, *19* (4), 2614-2619.
9. Zhang, N.; Wang, L.; Wang, H.; Cao, R.; Wang, J.; Bai, F.; Fan, H., Self-Assembled One-Dimensional Porphyrin Nanostructures with Enhanced Photocatalytic Hydrogen Generation. *Nano Letters* **2018**, *18* (1), 560-566.
10. Liao, P.; Hu, Y.; Liang, Z.; Zhang, J.; Yang, H.; He, L.-Q.; Tong, Y.-X.; Liu, J.-M.; Chen, L.; Su, C.-Y., Porphyrin-based imine gels for enhanced visible-light photocatalytic hydrogen production. *Journal of Materials Chemistry A* **2018**, *6* (7), 3195-3201.
11. Min, K. S.; Kumar, R. S.; Lee, J. H.; Kim, K. S.; Lee, S. G.; Son, Y.-A., Synthesis of new TiO₂/porphyrin-based composites and photocatalytic studies on methylene blue degradation. *Dyes and Pigments* **2019**, *160*, 37-47.
12. Lu, J.; Li, Z.; An, W.; Liu, L.; Cui, W., Tuning the Supramolecular Structures of Metal-Free Porphyrin via Surfactant Assisted Self-Assembly to Enhance Photocatalytic Performance. *Nanomaterials* **2019**, *9* (9), 1321.
13. La, D. D.; Bhosale, S. V.; Jones, L. A.; Bhosale, S. V., Arginine-induced porphyrin-based self-assembled nanostructures for photocatalytic applications under simulated sunlight irradiation. *Photochemical & Photobiological Sciences* **2017**, *16* (2), 151-154.
14. Aljabri, M. D.; La, D. D.; Jadhav, R. W.; Jones, L. A.; Nguyen, D. D.; Chang, S. W.; Tran, L. D.; Bhosale, S. V., Supramolecular nanomaterials with photocatalytic activity obtained via self-assembly of a fluorinated porphyrin derivative. *Fuel* **2019**, *254*, 115639.
15. Aljabri, M. D.; Gosavi, N. M.; Jones, L. A.; Morajkar, P. P.; La, D. D.; Bhosale, S. V., Arginine-Induced Self-Assembly of Protoporphyrin to Obtain Effective Photocatalysts in Aqueous Media Under Visible Light. *Molecules* **2019**, *24* (22), 4172.
16. Rao, H.; Lim, C.-H.; Bonin, J.; Miyake, G. M.; Robert, M., Visible-Light-Driven Conversion of CO₂ to CH₄ with an Organic Sensitizer and an Iron Porphyrin Catalyst. *Journal of the American Chemical Society* **2018**, *140* (51), 17830-17834.
17. Won, D.-I.; Lee, J.-S.; Ba, Q.; Cho, Y.-J.; Cheong, H.-Y.; Choi, S.; Kim, C. H.; Son, H.-J.; Pac, C.; Kang, S. O., Development of a Lower Energy Photosensitizer for Photocatalytic CO₂ Reduction: Modification of Porphyrin Dye in Hybrid Catalyst System. *ACS Catalysis* **2018**, *8* (2), 1018-1030.
18. Ishizuka, T.; Ohkawa, S.; Ochiai, H.; Hashimoto, M.; Ohkubo, K.; Kotani, H.; Sadakane, M.; Fukuzumi, S.; Kojima, T., A supramolecular photocatalyst composed of a polyoxometalate and a photosensitizing water-soluble porphyrin diacid for the oxidation of organic substrates in water. *Green Chemistry* **2018**, *20* (9), 1975-1980.
19. Spellane, P. J.; Gouterman, M.; Antipas, A.; Kim, S.; Liu, Y. C., Porphyrins. 40. Electronic spectra and four-orbital energies of free-base, zinc, copper, and palladium tetrakis(perfluorophenyl)porphyrins. *Inorganic Chemistry* **1980**, *19* (2), 386-391.
20. Magna, G.; Monti, D.; Di Natale, C.; Paollesse, R.; Stefanelli, M., The Assembly of Porphyrin Systems in Well-Defined Nanostructures: An Update. *Molecules (Basel, Switzerland)* **2019**, *24* (23), 4307.
21. Würthner, F.; Kaiser, T. E.; Saha-Möller, C. R., J-Aggregates: From Serendipitous Discovery to Supramolecular Engineering of Functional Dye Materials. *Angewandte Chemie International Edition* **2011**, *50* (15), 3376-3410.
22. La, D. D.; Hangarge, R. V.; V. Bhosale, S.; Ninh, H. D.; Jones, L. A.; Bhosale, S. V., Arginine-Mediated Self-Assembly of Porphyrin on Graphene: A Photocatalyst for Degradation of Dyes. *Applied Sciences* **2017**, *7* (6), 643.
23. Li, Q.; Zhao, N.; Bai, F., Size- and shape-dependent photocatalysis of porphyrin nanocrystals. *MRS Bulletin* **2019**, *44* (3), 172-177.
24. Hestand, N. J.; Spano, F. C., Expanded Theory of H- and J-Molecular Aggregates: The Effects of Vibronic Coupling and Intermolecular Charge Transfer. *Chemical Reviews* **2018**, *118* (15), 7069-7163.

TOC/graphics

